

Development of Lead Free Magnetolectric Materials for Magnetic Field Sensor Applications

A. Srinivas^{#,*}, N. Shara Sowmya[§], Pavan Kumar Naini[!], Partha Ghosal[#] and M. Manivel Raja[#]

[#]DRDO-Defence Metallurgical Research Laboratory, Kanchanbagh - 500 066, India

[§]Center for Materials for Electronics Technology, Thrissur - 680 581, India

[!]Department of Sciences and Humanities, Matrusri Engineering College, Hyderabad - 500 059, India

*E-mail: adirajs.dmrl@gov.in

ABSTRACT

(100-x) Na_{0.5}Bi_{0.5}TiO₃ (NBT)-(x) NiFe₂O₄ (NFO) (x = 0, 20, 40, 60, 80 and 100) composites are synthesized using conventional solid state reaction method. Crystal structure studies are performed by using X-ray Diffraction technique (XRD) and the Rietveld analysis of XRD patterns confirms the co-existence of cubic (NFO) and rhombohedral (NBT) symmetry with Fd-3m and R3c space groups, respectively. Micro-structural study reveals the formation of combination of composite phases and its inter-coupling grains. The average grain sizes and area percentage of each phase for the composites are calculated using Image J software. The Magnetisation versus Magnetic field (M-H) hysteresis loops show soft magnetic behavior of composites with variation in Saturation magnetization (M_S) and Coercivity (H_C). A maximum M_S (34 emu/g) and low H_C (15 Oe) is obtained for (80) NFO - (20) NBT composite. The Polarization – Electric field (P-E) analysis shows that the maximum saturation polarization (P_S) is obtained for (60)NBT-(40)NFO sample and is attributed to the leakage current generated by conductive NFO phase. The coupling between the ferrite and ferroelectric phase is studied based on the magnetolectric voltage coefficient (α_{ME}). The maximum (α_{ME}) of 1.82 mV/cm-Oe is obtained for (80)NBT -(20)NFO sample and this is almost 80% higher than the previously published literature on NBT-NFO composites. This can be attributed to the uniform distribution of grains with each ferroelectric phase surrounded by ferrite phase as shown in the morphological study.

Keywords: Magnetolectric coefficient; Ferrites; Piezoelectrics; Magnetolectric coupling

1. INTRODUCTION

Multiferroics are the novel multifunctional materials which exhibits two or more ferroic order parameters consisting of combinations such as Ferroelectric (FE), Ferromagnetic (FM) and ferroelastic¹⁻². Magnetolectric (ME) materials are the materials in which the coexistence of Ferroelectric (FE) and Ferromagnetic (FM) ordering occurs³. The advantage of this coexistence offers the best features in memory device applications, transducers, sensors, phase shifters, memory devices, resonators and tunable filters⁴⁻⁵.

In the naval applications, lots of sensors were used for degaussing as well as sensing the magnetic signatures. These lead-free magnetolectric composites have potential to use in the magnetic field sensor applications. The ME phenomenon can be classified into both single phase and composite materials based on the number of phases. The ME coefficient (α_{ME}) in single phase materials such as BiFeO₃ (α_{ME} = 7 mV/cm.Oe)⁶ Cr₂O₃ (α_{ME} = 0.74 mV/cm.Oe)⁷, exhibit intrinsic ME effect and it is due to the sub-lattice interactions in the single phase.

The limitation of single phase ME materials in practical applications is due to its low ME coupling which is occurring below the room temperature. Alternatively, in composite materials, the higher ME response is obtained when compared

with single phase materials⁸⁻¹⁰ due to the mechanical interaction between ferroelectric and ferromagnetic phases. The ME effect can be realized in two methods: (i) the electric polarization can be measured with varying magnetic field (direct ME) and (ii) the magnetization can be measured with varying electric field which is a converse ME effect.

The basic requirements for high ME output includes: no chemical reaction between the two ferroic orders, the resistivity of both the phases should be higher to avoid the leakage path of the charges and the magnitude of magnetostriction and piezoelectric coefficients should be high enough for efficient strain transfer¹¹. There are various reports based on lead based ME composites which exhibit higher ME output with excellent piezoelectric and electromechanical properties close to the Morphotropic Phase Boundary (MPB) composition. Such lead-based ME composites were discussed in many review articles¹²⁻¹⁴. In order to overcome the toxicity of lead to human beings, lead-free ME materials are developed whose properties are similar to that of lead based compounds¹⁵.

The lead free NBBT (Na_{0.5}Bi_{0.5}TiO₃-BaTiO₃) with epoxy¹⁶, BCZT (Ba_{0.85}Ca_{0.15})(Zr_{0.1}Ti_{0.9})O₃¹⁷ and Na_{0.5}Bi_{0.5}TiO₃ (NBT)¹⁸ exhibits excellent piezoelectric and ferroelectric properties near room temperature. NBT is one among the lead-free piezoelectric material with Ti⁴⁺ at B-site and Na⁺, Bi³⁺ ions at A-site which exhibits high remnant polarization,

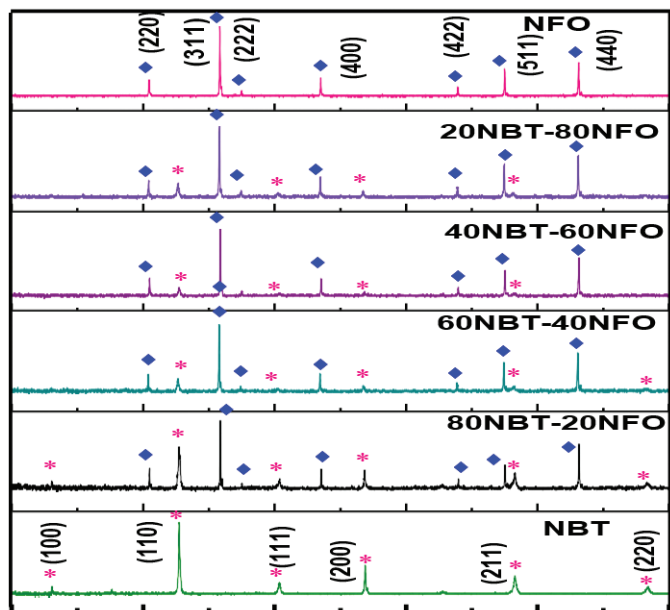


Figure 1. XRD patterns of $(100-x) \text{Na}_{0.5}\text{Bi}_{0.5}\text{TiO}_3$ - $(x) \text{NiFe}_2\text{O}_4$ ($x=0, 20, 40, 60, 80$ and 100) composite.

($P_r \sim 38 \mu\text{C}/\text{cm}^2$), coercive field ($E_C \sim 73 \text{ kV}/\text{cm}$) and Curie temperature ($T_C = 320 \text{ }^\circ\text{C}$). NBT exhibits rhombohedral ($R3c$) symmetry at room temperature. On the other hand, the high ME response also depends on the magnetostrictive phase with high permeability (μ) and strain sensitivity ($d\lambda/dH$). NiFe_2O_4 (NFO) is a soft-magnetic material with inverse spinel AB_2O_4 structure of Ni ions occupying A-site (tetrahedral) and Fe ions occupy both A and B (octahedral) sites. It exhibits low coercivity ($H_C \sim 100 \text{ Oe}$), large magnetostrictive coefficient (λ) of -35 ppm^{19} and high electrical resistivity (ρ) of the order of $3500 \text{ k}\Omega\text{-m}^{20}$.

In our previous study, the magnetic and electrical properties of BCZT-NFO were studied and obtained high α_{ME} of $13.3 \text{ mV}/\text{cm}\cdot\text{Oe}^{21}$. As per the literature reports, the α_{ME} of $0.22 \text{ mV}/\text{cm}\cdot\text{Oe}^{22}$ for $(0.10)\text{NiFe}_2\text{O}_4$ - $(0.90)\text{Na}_{0.5}\text{Bi}_{0.5}\text{TiO}_3$ composite and 0.14% for $(67)\text{NiFe}_2\text{O}_4$ - $(33)\text{Na}_{0.5}\text{Bi}_{0.5}\text{TiO}_3$ composite²³ has been observed. One can expect large ME effect in the NBT-NFO system, if there is a uniform distribution of both the piezo and ferromagnetic phases. To achieve this, proper precautions are considered during the sample preparation and are explained in this manuscript. In the present investigation,

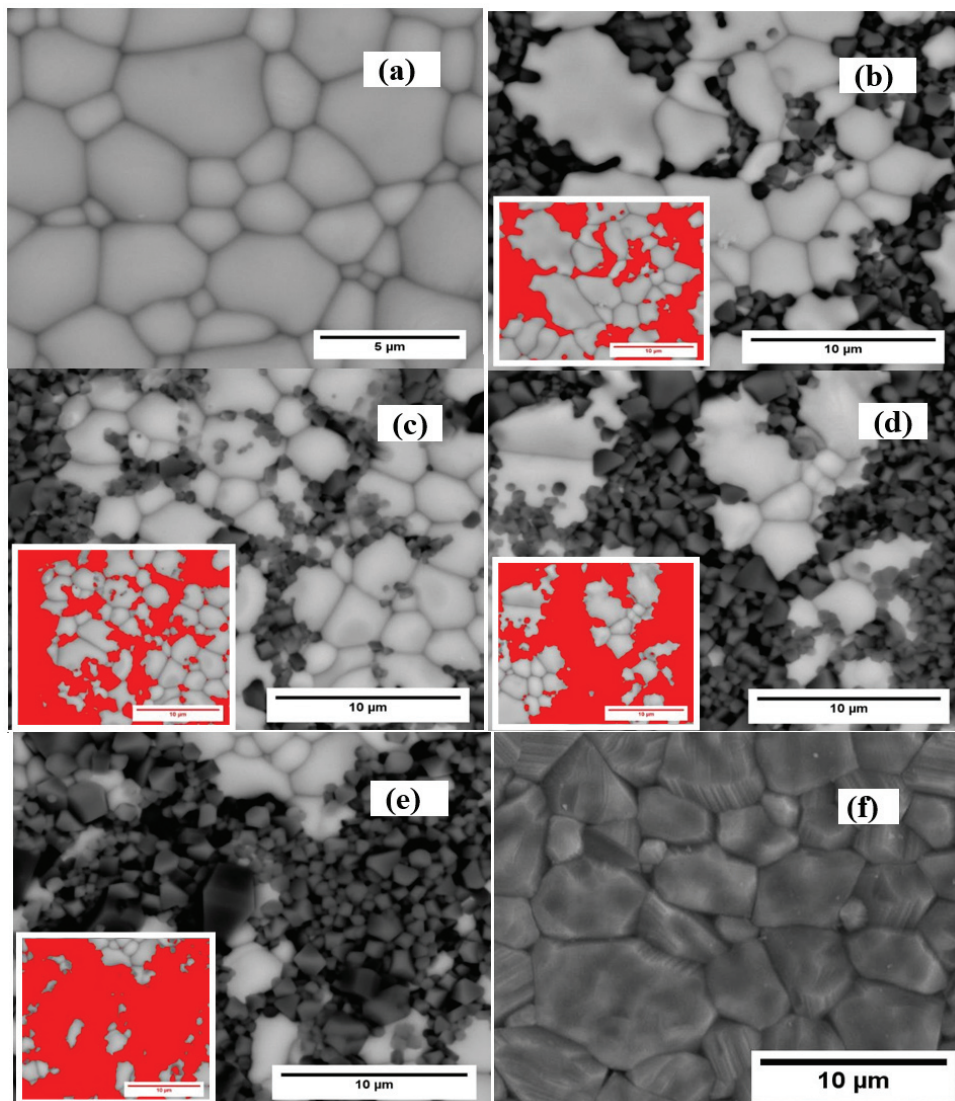


Figure 2: BSE images of (a) NBT (b) 80NBT-20NFO (c) 60NBT-40NFO, (d) 40NBT-60NFO, (e) 20NBT-80NFO (f) NFO samples.

composites of $(100-x)\text{Na}_0.5\text{Bi}_0.5\text{TiO}_3$ (NBT)- $(x)\text{NiFe}_2\text{O}_4$ (NFO) have been prepared and systematic study of magnetic, ferroelectric and magneto electric effect has been carried out and the results are presented here.

2. EXPERIMENTAL WORK

Magnetolectric $(100-x)\text{Na}_0.5\text{Bi}_0.5\text{TiO}_3$ - $(x)\text{NiFe}_2\text{O}_4$ ($x=0, 20, 40, 60, 80$ and 100) composites were synthesised using the solid state double reaction method. Stoichiometric amounts of Na_2CO_3 , Bi_2O_3 and TiO_2 (Sigma Aldrich, purity >99%) were weighed for synthesizing $\text{Na}_0.5\text{Bi}_0.5\text{TiO}_3$ (NBT). The powders were ball milled for 5h with low rpm and calcined at 800°C for 3 h in an air atmosphere. For the oxide based ceramic materials, solid state double sintering method will be adopted and it is well known sintering methodology. Usually, the calcination will be done around 800 - 900°C for all the oxide based ceramic materials. The calcination temperature will be decided based on the final sintering temperature. Usually, the calcination will be done about 200 to 250°C temperature lower than final sintering temperature. NBT final sintering temperature is in the range of 1000 - 1100°C . Hence, the calcination is carried out at 800°C . Similarly, NiFe_2O_4 (NFO) was synthesized by using NiO and Fe_2O_3 (Sigma Aldrich Grade, purity >99 %) as raw materials. These materials were ground well and milled for 5 h with low rpm and the powders are calcined at 1000°C for 5 h. The obtained calcined powders of NBT and NFO were mixed, ground and ball milled again for 2 h with low rpm in required proportions for the composites i.e., $80\text{NBT}-20\text{NFO}$, $60\text{NBT}-40\text{NFO}$, $40\text{NBT}-60\text{NFO}$ and $20\text{NBT}-80\text{NFO}$. Finally, the composite powders were sieved to attain uniform grain size. To attain efficient compaction, PVA binder (1 wt%) was added to the mixed powders of each composite and ground for 1 h until it gets dry. The obtained powders are again sieved for achieving uniform distribution of powder particles before compaction. Circular pellets with 10mm diameter and ~ 1 - 1.5 mm thickness were prepared by applying a pressure of 150 MP and finally the composites were sintered at 1050°C for 2 h in air atmosphere.

The structural studies of NBT-NFO composites at room temperature are measured using X-Ray Diffractometer (PHILIPS 3121) with a diffraction angle 2θ ranging from 20° to 90° at a scanning rate of $2^\circ/\text{min}$ by using $\text{Cu-K}\alpha$ ($\lambda = 1.54058\text{\AA}$) radiation. The obtained XRD data is further analysed using Fullprof Rietveld Refinement program. Backscattered electron (BSE) images were recorded with a Scanning Electron Microscope (SEM) of LEO 440 for micro-structural studies. The average grain sizes of each composite and its distribution is calculated using Image J software. The room temperature magnetic properties are studied by using Vibrating Sample Magnetometer (VSM, EV9 ADE Model, USA). The standard FE loop tester (aixACCT TF Analyser 2000) was used to measure P-E hysteresis loops at 1 Hz. The electrical poling around 30 min is applied to the composites in the electric field range of 2 - 5 kV/mm with varying the composition. The ME measurement of the poled composites are performed in longitudinally magnetized and transversely polarized (L-T) mode which correspond to aE_31 by placing the samples in between the poles of DC magnets. The induced voltage across

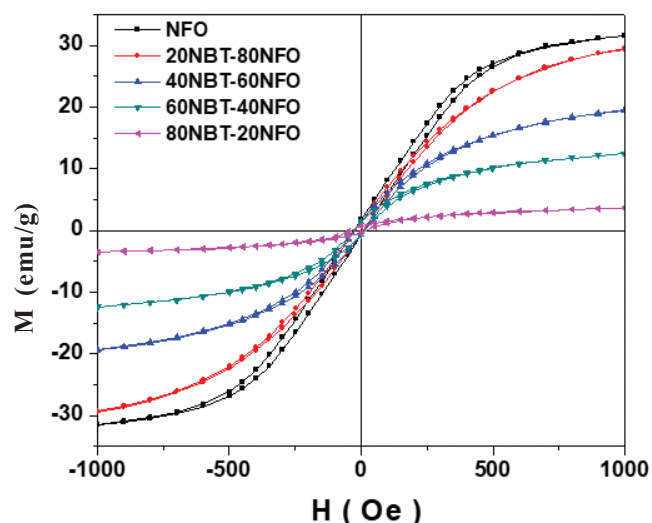


Figure 3. M-H graph of $(100-x)\text{Na}_0.5\text{Bi}_0.5\text{TiO}_3$ - $(x)\text{NiFe}_2\text{O}_4$ ($x = 20, 40, 60, 80$ and 100) composites.

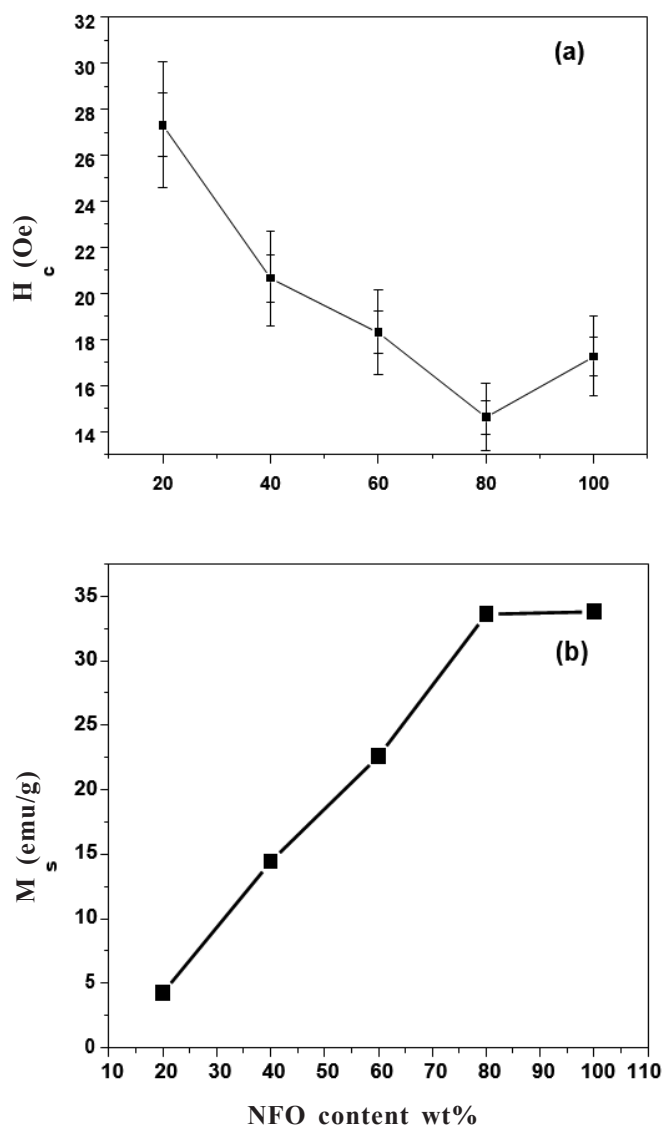


Figure 4. Comparison of coercivity and magnetic saturation with NFO wt% for $(100-x)\text{Na}_0.5\text{Bi}_0.5\text{TiO}_3$ - $(x)\text{NiFe}_2\text{O}_4$ ($x = 0, 20, 40, 60, 80$ and 100).

the composites is measured using a lock-in amplifier (SR 830) with respect to H_{dc} in presence of $H_{ac} = 1$ Oe at 1 kHz representing off-resonance ME measurements.

3. RESULTS AND DISCUSSION

3.1 X-ray Diffraction Analysis

The XRD patterns of $(100-x) \text{Na}_0.5\text{Bi}_0.5\text{TiO}_3 - (x) \text{NiFe}_2\text{O}_4$ ($x=0, 20, 40, 60, 80$ and 100) are shown in Fig. 1. The XRD peaks of all the samples are indexed with their corresponding Miller indices. Two sets of well-defined peaks are observed in the composite samples. No extra

phases are observed, which suggests that there could be no chemical interaction at the NBT-NFO interface during sintering. NFO shows single phase cubic crystal structure with a space group of $Fd-3m$ and NBT exhibit rhombohedral crystal structure with a space group of $R3c$. The observed XRD pattern shows that the peak intensity increases with increase in NFO content for NFO phase, whereas it decreases for NBT phase. For $x=40, 60$ and 80 samples, the peak intensity of NBT phase at 23.1° and 68.3° is very less. The maximum intensity peak for NFO and NBT is observed at 35.7° and 32.6° respectively, for the composites $(100-x) \text{Na}_0.5\text{Bi}_0.5\text{TiO}_3 - (x) \text{NiFe}_2\text{O}_4$ ($x=20, 40, 60$ and 80).

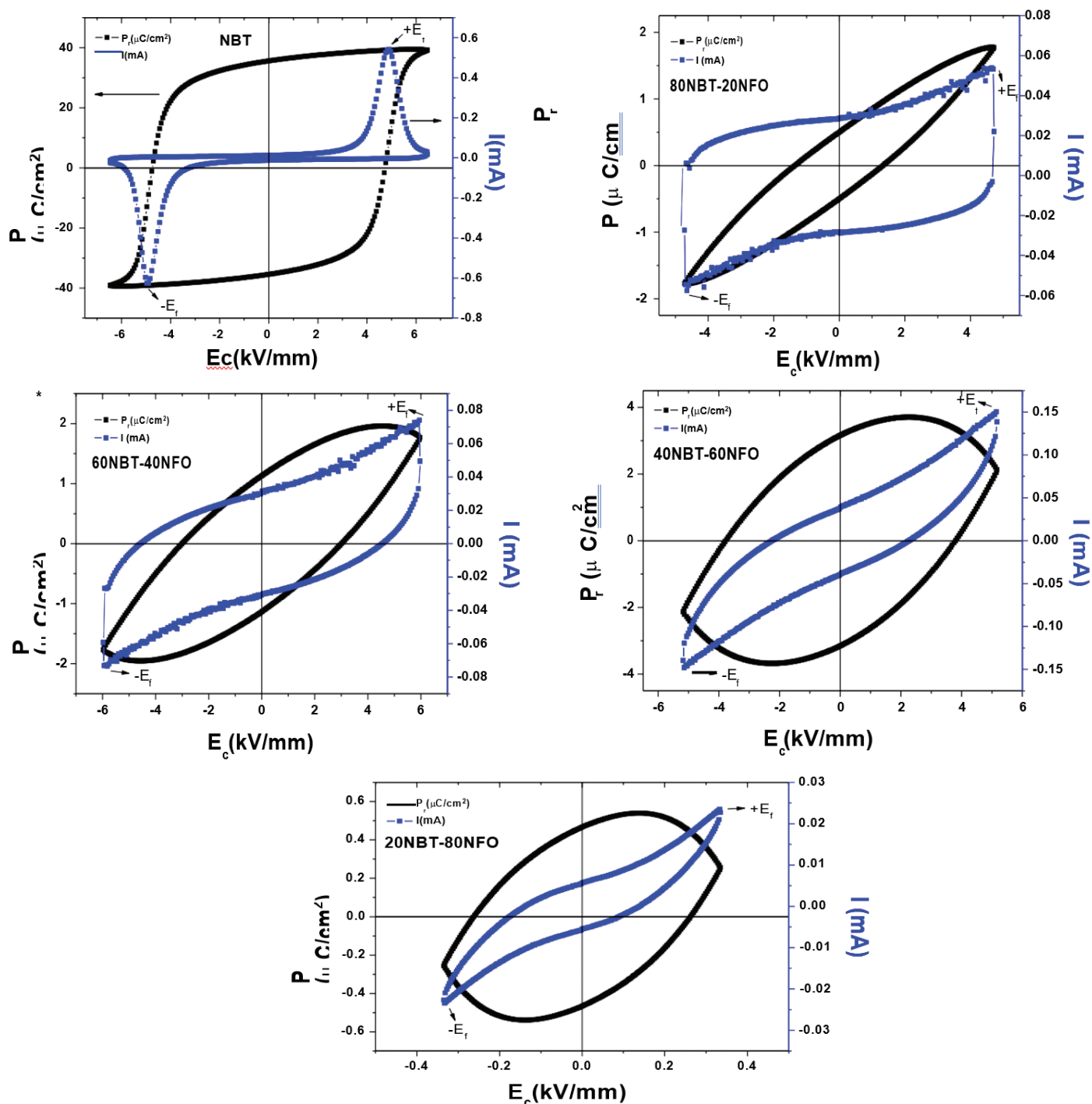


Figure 5. P-E loops of $(100-x) \text{Na}_0.5\text{Bi}_0.5\text{TiO}_3 - (x) \text{NiFe}_2\text{O}_4$ ($x=20, 40, 60$ and 80) composites.

3.2 SEM Analysis

The surface morphological studies of the composites $(100-x) \text{Na}_0.5\text{Bi}_0.5\text{TiO}_3 - (x) \text{NiFe}_2\text{O}_4$ ($x=0, 20, 40, 60, 80$ and 100) are shown in Fig. 2. All the composites show homogeneous and highly dense microstructure. From the Archimedes principle, all the composite samples showed bulk density of 5.4 g/cc for NFO and 5.96 g/cc for NBT, which is 85-90% of the theoretical density. It can be observed from the microstructure, that there is a uniform distribution of both the phases where each ferroelectric phase (NBT) is surrounded by ferrite phase (NFO) indicating a strong inter-coupling between the two phases. The grain to grain contact ensures effective transfer of strain from ferrite to the ferroelectric phase. As shown in Fig. 2, the brighter phase (white) represents NBT with larger grain size and NFO (black) as the dark phase with smaller grain size. The average grain size values for $x=0$ (NBT) and 100 (NFO) samples were found to be 3.8 and $2.2 \mu\text{m}$, respectively. The average grain size and the area of the NFO phase is increasing with the increase in the NFO wt%, whereas for NBT phase the average grain size and area decreases. The area percentage obtained for each phase matches well with that of initially considered compositions for the composites. The NFO phase in all the composites is highlighted with red color and is shown in the inset of Fig. 2.

3.3 Magnetization Studies

Magnetisation (M) - Magnetic field (H) hysteresis plots for the composites $(100-x) \text{Na}_0.5\text{Bi}_0.5\text{TiO}_3 - (x) \text{NiFe}_2\text{O}_4$ ($x=20, 40, 60, 80$ and 100) are shown in Fig. 3. The loops confirm the ferrimagnetic nature of the samples. The variation of Coercivity (H_c) and Saturation Magnetisation (M_s) as a function of the NFO content are plotted in Fig. 4 (a) and (b). The co-existence of non-magnetic NBT phase is likely to influence the magnetic properties of the composites. It can be seen from the Fig. 4(b), that the value of M_s is found to increase with an increase in the NFO content and magnetization has attained saturation at an applied magnetic field of $\sim 1000 \text{ Oe}$ for all the composites. The reason for increase in M_s can be attributed to increase in magnetic dipole moment (μB) with NFO concentration. Similarly, H_c values decreases with the increase in the NFO content up to $x=80 \text{ wt\%}$ composite and slight increase in H_c is observed for pure NFO. This is due to the domain wall pinning caused by non-magnetic NBT (perovskite phase) on magnetic moments of NFO at magnetic or ferroelectric phase interfaces. As a result, magnetic dipoles of NFO phases are constrained by the ferroelectric phase and are unable to switch freely in the composites. The structural defects and the domain boundaries may also contribute to the pinning.

3.4 Ferroelectric (P-E) Analysis

The polarization-electric field (P-E) and current-electric field (I-E) loops of the composites $(100-x) \text{Na}_0.5\text{Bi}_0.5\text{TiO}_3 - (x) \text{NiFe}_2\text{O}_4$ ($x=0, 20, 40, 60$ and 80) are shown in Fig. 5, indicating the typical ferroelectric nature of the samples. The observed loops in Fig. 5 for all the composites represent the lossy behavior. The previous literature studies on $(0.5\text{BZT}-$

$0.5\text{BCT})-(100-x) \text{NiFe}_2\text{O}_4^{21}$, $(\text{Na}_0.5\text{Bi}_0.5)\text{TiO}_3-\text{BaTiO}_3-\text{CoFe}_2\text{O}_4^{24}$ and $(100-x)\text{Na}_0.5\text{Bi}_0.5\text{TiO}_3-(x)\text{CoFe}_2\text{O}_4^{25}$ composites had shown the lossy behavior and attributed to the leakage arising from NiFe_2O_4 phase. In the present study, the similar loops are observed and this behavior can also be attributed to the leakage current arising from NFO (ferrite) phase.

It can be seen from Fig. 6, that the P_r and P_s values are found to increase with an increase in NFO content till $x=60 \text{ wt\%}$ and with further increase in NFO content, P_s and P_r values are found to decrease. This can be due to i) the pinning effect caused in the NBT phase by the NFO phase and ii) leakage current generated by the conductive NFO phase. The E_C values are found to increase till $x=60 \text{ wt\%}$ and it decreases for $x=80 \text{ wt\%}$. This can be attributed to the hindrance caused to the spontaneous polarization reversal of ferroelectric domains due to the pinning effect caused by the oxygen vacancies which are formed during sintering²³. The depolarizing field created due to the spontaneous polarization in NBT can be compensated with the charges at the interface or surface. The threshold electric field of $+E_F$ and $-E_F$ represents two current peaks in I-E loops. The domain switching behavior in NBT ceramics is indicated by the loading and unloading cyclic electric fields, representing the intrinsic ferroelectric nature of the composites. At this stage it is pertinent to discuss the reason for pinning effect caused in the NBT phase by the NFO phase influences P_s and P_r values. The values of Remnant polarization (P_r) and Saturation polarization (P_s) increased with increase in NFO content due to the pinning of the NBT domain wall by the conductive NFO phase. The mechanism driving the ferroelectric ordering in NBT and magnetic ordering in NFO is quite different. Long-range dipolar interactions are mainly responsible for exhibiting the ferroelectric nature. In the NBT-NFO composites, with increase in NFO concentration, the long-range ferroelectric ordering gets disturbed which is clearly evident from the BSE images (Fig. 2). Hence the NBT domain wall gets pinned and cannot move with further increase in electric field.

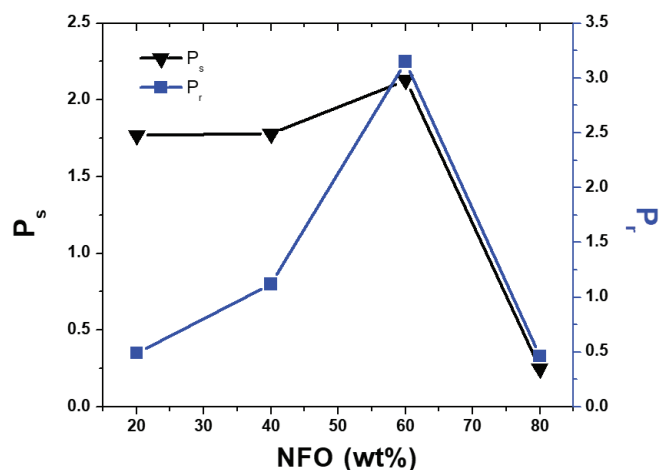


Figure 6. Comparison of saturation polarization, remnant polarization with NFO wt% for $(100-x) \text{Na}_0.5\text{Bi}_0.5\text{TiO}_3 - (x) \text{NiFe}_2\text{O}_4$ ($x=0, 20, 40, 60, 80$ and 100).

3.5 Magnetolectric (M-E) Analysis

The most essential property of multiferroic materials is to measure the cross coupling effect (Magnetolectric effect).

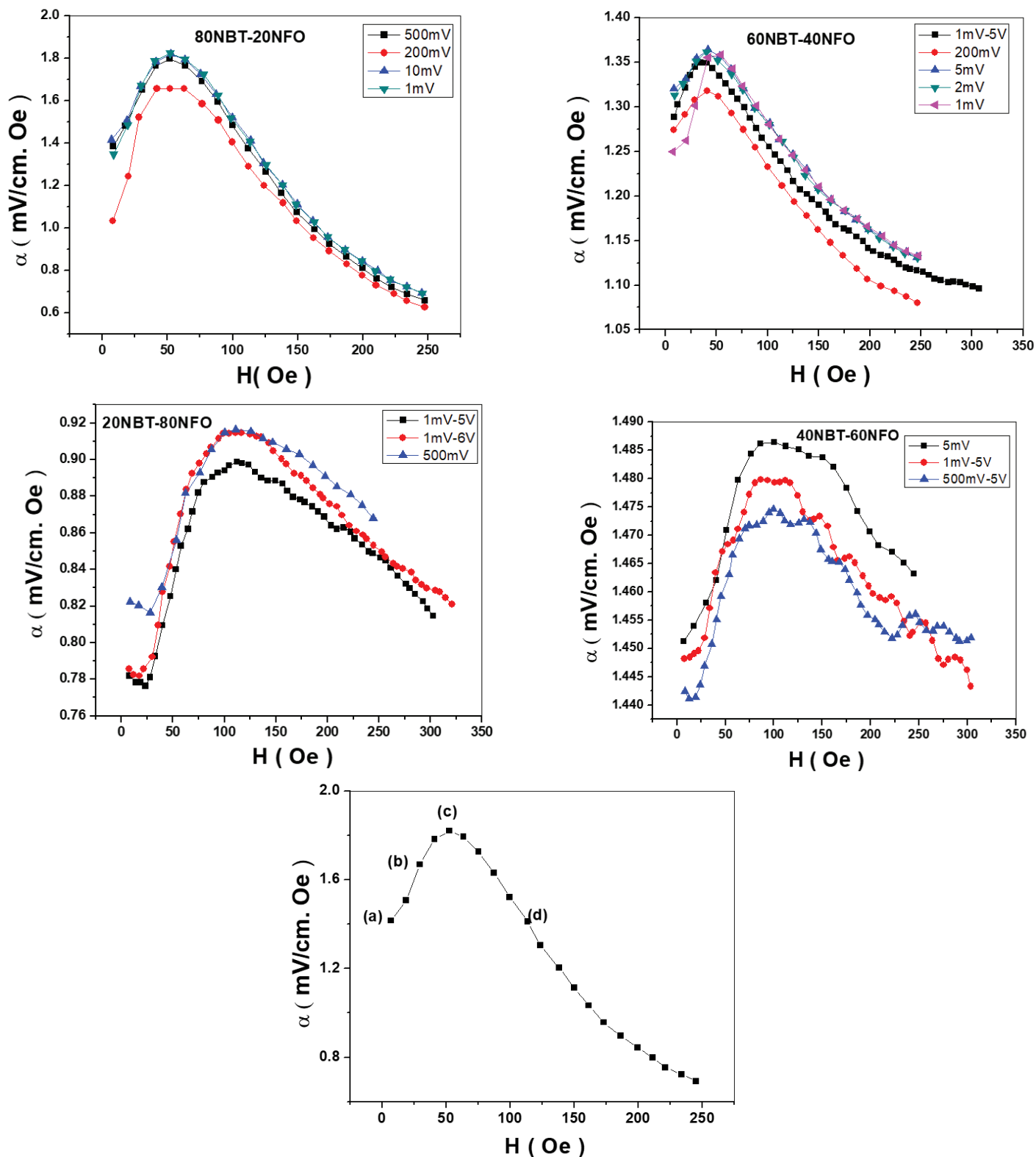


Figure 7. M-E curves of $(100-x) \text{Na}_{0.5}\text{Bi}_{0.5}\text{TiO}_3 - (x) \text{NiFe}_2\text{O}_4$ ($x=20, 40, 60, 80$) composites at different sensitivities.

The ME voltage coefficient, α_{ME} used for determining the coupling between the electric and magnetic dipole interactions

was given by the relation, $\alpha_{\text{ME}} = \frac{\delta E}{\delta H * t}$ where 'E' is an electric field, 'H' is the magnetic field and 't' is the thickness of the sample. The induced voltage is measured in the poled direction

for all the composites. In the present study, α_{31} for the composites $(100-x) \text{Na}_{0.5}\text{Bi}_{0.5}\text{TiO}_3 - (x) \text{NiFe}_2\text{O}_4$ ($x = 20, 40, 60, 80$) at 1 kHz frequency as a function of d.c magnetic field (H_{dc}) at a fixed H_{ac} of 1Oe has been measured and the results are shown in Fig. 7. The deformation in the ferroelectric phase is due to the magnetostrictive nature of magnetic material

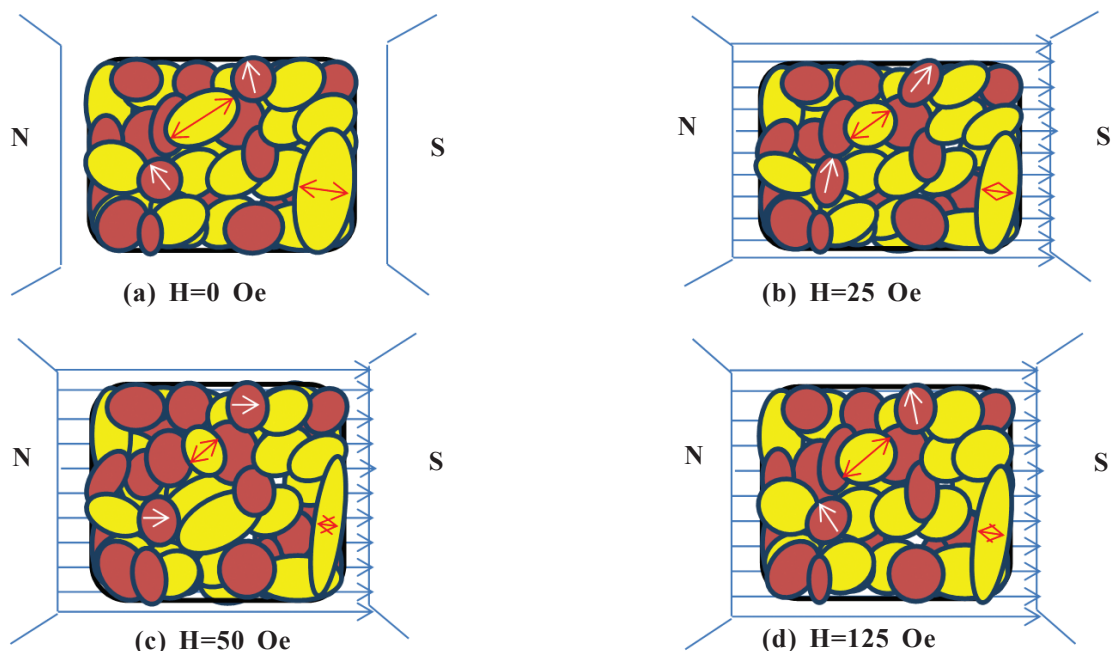


Figure 8. Pictorial representation of NFO and NBT domain. Domains in yellow color represents NBT and brown color represents NFO.

Table I. Parameters from Image J of $(100-x) \text{Na}_{0.5}\text{Bi}_{0.5}\text{TiO}_3 - (x) \text{NiFe}_2\text{O}_4$ ($x=20, 40, 60$ and 80) composites

	80 NBT-20 NFO		60 NBT-40 NFO		40 NBT-60 NFO		20 NBT-80 NFO	
	NBT	NFO	NBT	NFO	NBT	NFO	NBT	NFO
Area (μm^2)	443.31	116.78	331.57	223.15	214.05	331.85	105.980	376.043
Average Size (μm)	3.9	0.92	3.34	1.73	2.52	2.35	0.288	3.5
Area (%)	79.15	20.85	59.498	40.043	39.211	60.789	22.25	77.533
Total area (μm^2)	560.1		554.72		545.9		482.023	

Table 2. Comparison of ME coefficient with literature for NBT-NFO composite system

Composition	Magnetolectric coefficient	References
$(0.10)\text{NiFe}_2\text{O}_4 - (0.90)\text{Na}_{0.5}\text{Bi}_{0.5}\text{TiO}_3$	0.22 mV/cm. Oe	Tanvi Bhasin ²² , <i>et al.</i>
$(67)\text{NiFe}_2\text{O}_4 - (33)\text{Na}_{0.5}\text{Bi}_{0.5}\text{TiO}_3$	0.14 mV/cm. Oe	Narendra babu ²³ , <i>et al.</i>
$(80)\text{Na}_{0.5}\text{Bi}_{0.5}\text{TiO}_3 (20)\text{NiFe}_2\text{O}_4$	1.82 mV/cm. Oe	Present study

under the influence of external magnetic field, causing a change in electric polarization when mechanically coupled with piezoelectric phase representing magnetolectric effect, αME . The ME coefficient depends upon the composition, mechanical coupling and mole fraction of two phases. There is no much variation in the induced ME coefficient obtained at different sensitivities in all the samples as seen from the Fig. 7. In all the composites, the ME coefficient increases with an increase in the magnetic field, since the magnetostrictive strain rates increased with increasing field. Beyond a certain field, the magnetostriction gets saturated producing a constant electric field. With further increase in the field, it results in the ME coefficient to decrease continuously²⁶. It can also be attributed to the leakage path arising at NBT phase due to the low resistivity of the NFO phase²¹. A maximum ME voltage coefficient of 1.82 mV/cm.Oe is obtained for 80NBT-20NFO

composite which is attributed to the uniform distribution of NFO and NBT phases shown in Fig. 4 and facilitated effective strain transfer leading to a high ME response. The ME coefficient observed by Tanvi Bhasin *et al.*²² for the composite $(0.90)\text{Na}_{0.5}\text{Bi}_{0.5}\text{TiO}_3 - (0.10)\text{NiFe}_2\text{O}_4$ was 0.22mV/cm-Oe. The other report on $(33)\text{Na}_{0.5}\text{Bi}_{0.5}\text{TiO}_3 - (67)\text{NiFe}_2\text{O}_4$ ²³ had shown the ME output of 0.14%. Therefore, ME coefficient obtained in the present study is higher than the previously reported values on NBT-NFO composites. The comparison of ME coefficient values for NBT-NFO composite system with previously published literature is shown in Table 1.

In order to understand the origin of ME behavior in these composites, a schematic representation has been made for (80) NBT-(20) NFO sample and is shown in Fig. 8. The schematic representation is considered by assuming NBT and NFO shape as spherical. In Fig. 8, NBT domain is represented

with yellow color and NFO with brown color. At $H = 0$ Oe (shown in Fig. 8(a)), the NFO magnetic domains are aligned in random direction. It is well known that Nickel ferrite exhibits negative magnetostriction of -32 ppm¹⁹ in which the dimensions of a body contract with the application of magnetic field. In (80) NBT- (20) NFO sample, with the application of magnetic field of 25 Oe, the NFO domains try to align to reduce its dimensions²⁷. During this process, the NBT domains which are in between the NFO domains gets effected by the magneto-elastic stresses as shown in Fig. 8(b). This stresses will produce a net charge in the NBT indicating the elasto-electric interactions in the composites. In Fig. 8(b), the NBT domains suffered by magneto-elastic stresses and produces elasto-electric fields resulting in coupling (or magnetoelectric coupling). On further application of field of 50 Oe i.e., at H_{max} , NFO exhibits maximum magnetostriction where all the NFO domains aligned and NBT domains affected to its maximum to produce maximum charge or voltage as shown in Fig. 8(c). With further application of field to 125 Oe (shown in Fig. 8(d)), the NFO and NBT domains return to random state and become free from magneto-elastic stresses as discussed in our previous study²⁶. Therefore, the maximum ME coefficient for NBT-NFO system is obtained at higher concentrations of NBT i.e., for (80)NBT-(20)NFO sample. The observed ME output in the present study for the composite system NBT-NFO could be an effective magneto- electric composite used in low magnetic field sensor applications.

4. CONCLUSIONS

For any ME device applications, the piezoelectric and ferrimagnetic material properties are equally important. Particularly, in case of ME composites, effective strain transfer is the crucial factor to attain higher ME response. In this present study, a systematic variation of $\text{Na}_0.5\text{Bi}_0.5\text{TiO}_3\text{-NiFe}_2\text{O}_4$ composites were synthesized using the solid state reaction method. Sintered composites at 1020 °C for 2 h resulted in a sintered density of ~85-90 % of the theoretical density. XRD studies revealed the co-existence of two phases without any traces of impurities. BSE studies show the uniform distribution and good connectivity between the NBT and NFO phases. The high ME coefficient (α_{ME}) of 1.82 mV/cm-Oe was obtained for $x=80$ wt% composite, which is almost 80% higher than the previously reported values on NBT-NFO based composites. Hence, this investigation delivers a paradigm for synthesizing high performance NBT-NFO composites and could be an efficient lead-free ME composites for magnetic field sensor applications.

REFERENCES

- Eerenstein, W. Mathur, N.D. & Scott, J.F. Multiferroic and Magnetoelectric materials. *Nat.(Lond.)*, 2006, **442**, 759.
doi:10.1038/nature05023.
- Fiebig, M. Revival of the magnetoelectric effect. *J. Phys. D: Appl. Phys.*, 2005, **38**, R123-R152.
doi: 10.1088/0022-3727/38/8/R01.
- Schmid, H. Multi-ferroic Magnetoelectrics. *Ferroelectrics.*, 1994, **162**, 317-338.
doi:10.1080/00150199408245120.
- Scott, J.F. Multiferroic memories. *Nat. Mater.*, 2007, **6**, 256–257.
doi:10.1038/nmat1868.
- Ramesh, R. & Spaldin, Nicola A. Multiferroics: Progress and prospects in thin films. *Nat. Mater.*, 2007, **6**, 21–29.
doi:10.1038/nmat1805.
- Caicedo, J.M.; Zapata, J.A.; Gomez, M.E. & Prieto, P. Magnetoelectric coefficient in BiFeO_3 compounds. *J. Appl. Phys.*, 2008, **103**, 07E306.
doi: 10.1063/1.2839276.
- Wiegelmann, H.; Jansen, G.M. & Wyder, P. Magnetoelectric effect of Cr_2O_3 in strong static magnetic fields. *Ferroelectrics.*, 1994, **162**(1),141-146.
doi:10.1080/00150199408245099.
- Ryu, J.; Carazo, A.V.; Uchino, K. & Kim, H.E. Magnetoelectric properties in piezoelectric and magnetostrictive laminate composites. *Jpn. J. Appl. Phys.*, 2001, **40**, 4948.
doi: 0.1143/JJAP.40.4948.
- Islam, R.A. & Priya, S. Enhanced magnetoelectric effect in $(1-x)\text{Pb}(\text{Zr}_{0.52}\text{Ti}_{0.48})\text{O}_3 - (x)\text{NiFe}_{1.9}\text{Mn}_{0.1}\text{O}_4$ particulate composites electrical and magnetic properties. *Integrated Ferroelectr.*, 2006, **82**(1), 124.
doi: 10.1080/10584580600872976.
- Suryanarayana, S.V. Magnetoelectric interaction phenomena in materials. *Bull. Mater. Sci.*, 1994, **17**(7), 1259-1270.
doi: 10.1007/BF02747225.
- Van Den Boomgaard, J.; Van Run, A.M.J.G. & Van Suchtelen, J. Magnetoelectricity in piezoelectric-magnetostrictive composites. *Ferroelectrics.*, 1976, **10**(1), 295-298.
doi: 10.1080/00150197608241997.
- Haribabu Palneedi, V.A.; Shashank, Priya & Jungho, R. Status and perspectives of multiferroic magnetoelectric composite materials and applications. *Actuators.*, 2016, **5**(9), 5010009.
doi:10.3390/act5010009.
- Zhengyu, Ou; Caijiang, Lu; Aichao, Yang.; Hai, Zhou; Zhongqing, Cao; Renren, Zhu & Hongli, Gao. Self-biased magnetoelectric current sensor based on $\text{SrFe}_{12}\text{O}_{19}/\text{FeCuNbSiB/PZT}$ composite. *Sensors and Actuators A.*, 2019, **290**, 8–13.
doi: 10.1016/j.sna.2019.03.008
- Zhaoqiang, Chu; Mohammad Javad, Pourhosseini & Shuxiang, Dong. Review of multi-layered magnetoelectric composite materials and devices applications. *J. Phys. D: Appl. Phys.*, 2018, **15**, 243001.
doi: 10.1088/1361-6463/aac29b.
- Indrani, Coondoo; Joao, Vidal; Igor, Bdikin; R, Surmenev & Andrei, Kholkin. Magnetoelectric coupling studies in multiferroic $(\text{Ba}_{0.85}\text{Ca}_{0.15})(\text{Zr}_{0.1}\text{Ti}_{0.9})\text{O}_3 - (\text{Ni}_{0.7}\text{Zn}_{0.3})\text{Fe}_2\text{O}_4$ ceramic composites. *Ceramics Int.*, 2022, **48**, 24439-24453.
doi: 10.1016/j.ceramint.2022.05.052
- Xun, Zhou; Qingwen, Yue; Qiaozhen, Zhang; Jinpeng, Ma; Mingzhu, Chen; Jushan, Wang; Feifei, Wang;

- Yanxue, Tang; Di, Lin; Haosu, Luo & Xiangyong, Zhao. Preparation and simulation of lead free NBBT/epoxy 1–3 piezoelectric composites for high frequency medical ultrasound. *Composite Commun.*, 2022, **36**, 101399
doi: 10.1016/j.coco.2022.101399
17. Srinivas, A.; Krishnaiah, R.V.; Niranjan, V.L.; Kamat, S.V.; Karthik, T. & Saket Asthana. Ferroelectric, piezoelectric and mechanical properties in lead free (0.5)Ba(Zr_{0.2}Ti_{0.8})O₃ – (0.5) (Ba_{0.7}Ca_{0.3})TiO₃. *Ceramics Int.*, 2015, **41**, 1980–1985.
doi: 10.1016/j.ceramint.2014.08.127.
 18. Smolenskii, G.A.; Isupov, V.A.; Aganovskaya, A.I. & Krainik, N.N. *J. Atom-Economic reaction: Preparation and mechanism of Nano-SrB₂O₄ by solid-state reaction. Sov. Phys. Solid State.*, 1961, **2**, 2651.
doi:10.4236/sn.2011.14020.
 19. R. Grossinger, R.; Sato, Turtelli & N., Mehmood, Materials with high magnetostriction. *Mater. Sci. Eng.*, 2014, **60**, 012002.
doi: 10.1088/1757-899X/60/1/012002.
 20. P.I., Slick. *In: Wolforth EP Ferromagnetic materials, Vol 2*, 1980, North Holland, Amsterdam, 196.
doi: 10.1002/crat.19810160127.
 21. Shara, S.N.; Srinivas, A.; Reddy, V.G.; Praveen, K.P.; Das, J.D.; Kumar, D.; Subramanian, S.V. & Kamat, S.V. Magnetolectric coupling studies on (x) (0.5BZT-0.5BCT) – (100-x) NiFe₂O₄ [x = 90 -70 wt%. particulate composite. *Ceram. Int.*, 2016, **16**, S0272-8842.
doi: 10.1016/j.ceramint.2016.11.054.
 22. Bhasin, T.; Agarwal, A.; Sanghi, S.; Kotnala, R.K.; Shah, J.; Yadav, M. & Tuteja, M. Crystal structure, dielectric, magnetic and magnetolectric properties of xNiFe₂O₄-(1-x)Na_{0.5}Bi_{0.5}TiO₃ composites. *J. Alloys. Compounds.*, 2018, **18**, 0925-8388.
doi: 10.1016/j.jallcom.2018.03.219.
 23. Babu, N.; Jen-Hwa Hsu, S.; Chen, Y.S. & Lin, J.G. Magnetolectric response in lead-free multiferroic NiFe₂O₄-Na_{0.5}Bi_{0.5}TiO₃ composites. *J. Appl. Phys.*, 2011, **109**, 07D904.
doi: 10.1063/1.3540623.
 24. Venkata Ramana, E.; Figueiras, F.; Graçaa, M.P.F. & Valentea, M.A. Observation of magnetolectric coupling and local piezoresponse in modified (Na_{0.5}Bi_{0.5})TiO₃-BaTiO₃-CoFe₂O₄ lead-free composites. *Dalton Trans.*, 2014, **43**, 9934.
doi: 10.1039/C4DT00956H.
 25. Krishnaiah, R.V.; Srinivas, A.; Kamat, S.V.; Karthik, T. & Asthana, S. Effect of CoFe₂O₄ mole percentage on multiferroic and magnetolectric properties of Na_{0.5}Bi_{0.5}TiO₃/CoFe₂O₄ particulate composites. *Ceram. Int.*, 2014, **40**, 7799-7804.
doi: 10.1016/j.ceramint.2013.12.123.
 26. Srinivas, A.; Krishnaiah, R.V.; Karthik, T.; Suresh, P.; Asthana, S. & Kamat, S.V. Observation of direct and indirect magnetolectricity in lead free ferroelectric (Na_{0.5}Bi_{0.5}TiO₃)-magnetostrictive (CoFe₂O₄) particulate composite. *Appl. Phys. Lett.*, 2012, **101**, 082902.
doi: 10.1063/1.4745840.
 27. Cullity, B.D. & Graham, C.D. Introduction to magnetic materials. IEEE Press, John Wiley and Sons, 2009. 241.
doi: 10.1002/9780470386323.

CONTRIBUTORS

Dr Adiraj Srinivas is working as Scientist at DRDO-DMRL, Hyderabad. He obtained his PhD from Osmania University, Hyderabad. He is having expertise in the design and development of smart materials based on Multiferroic-Magnetolectrics and in the development of Microwave/Radar Absorbing Materials for stealth technology.

His contribution to the current study includes conceptualization, planning of experiments, carrying out experiments, test results, analysis, manuscript draft and manuscript reviews.

Dr N. Shara Sowmya is a Research Scientist at Center for Materials for Electronics Technology, Thrissur, Kerala. She obtained PhD from NIT, Warangal. Her research interests include the study of ferroelectric and piezoelectric properties of lead/lead-free materials for non-resonant impact, and actuator applications.

For the current study, she was involved in carrying out experiments, test results, analysis, manuscript draft, and manuscript reviews

Dr Pavan Kumar Naini works as Assistant Professor of Physics in the Department of Sciences and Humanities, Matrusri Engineering College, Hyderabad, India. His current research interests are synthesis and characterization of single phase and composite based Multiferroics for sensors, low-temperature magnetic refrigeration applications. He has expertise in ferrites and CMR manganites.

For the current study, he was involved in test results, analysis

Dr Partha Ghosal is working as Senior Scientist at DRDO-DMRL, Hyderabad. His contributions ranging from innovative basic research of international repute is in the advanced characterization techniques and sustained activities on research & development, characterization and testing of nano and advanced materials, specially Ti based composites and nano composites.

For the current study, he has provided support for data acquisition and test equipment. He has also given valuable suggestions and guidance to carry out this study.

Dr M. Manivel Raja is a Senior Scientist at DRDO-DMRL, Hyderabad. He obtained his PhD from University of Madras, Chennai. His area of research involve research and development of magnetic thin film sensors and spintronic devices.

For the current study, he has provided support for data acquisition and test equipments, given valuable suggestions and guidance to carryout this work.